J. Fluid Mech. (1973), *vol.* 60, *part* 1, *pp.* 63–79
Printed in Great Britain

The decay of perturbations in an electrically conducting and thermally radiating gas

By M. SRINIVASA SARMA AND L. V. K. V. SARMA
Department of Mathematics, Indian Institute of Technology, Madras

(Received 23 February 1973)

The decay of perturbations in an infinite, thermally radiating gas of perfect electrical conductivity in the presence of magnetic field is studied. Complete solutions for the decay of initial sinusoidal perturbations in the temperature, gas velocity and pressure are determined. The sinusoidal perturbations are superposed to yield solutions for the decay of initial 'step' temperature profiles consisting of a constant initial temperature perturbation inside a finite planar region, with zero temperature perturbation outside. For a broad range of small and intermediate Boltzmann numbers the cooling proceeds in time from being a constant-density cooling process to being a constant-pressure cooling process. The magnetic field causes slower temperature decay with time and makes the temperature perturbations tend to attain constant-pressure cooling values. It quickens the decay of velocity and pressure perturbations and thus the transition from a constant-density to a constant-pressure cooling process is hastened. This transition is produced by the magneto-acoustic waves generated near the profile edges by the radiative cooling.

1. Introduction

On account of the high ambient temperatures that prevail in many phenomena, it is of interest to consider the effects of thermal radiation in gasdynamics. The decay of perturbations in a radiating gas has been the subject of a number of previous investigations. Consideration of a sinusoidal disturbance proportional to $\exp\{i(\omega t - kx)\}$ leads to a characteristic equation which yields ω roots for a fixed wavenumber k, or k roots for a fixed frequency ω. The analyses of the k roots of the characteristic equation (spatially damped case) were carried out by Prokof'ev (1957), Riazantsev (1959) and Vincenti & Baldwin (1962). In addition to solving the characteristic equation for the k roots, Vincenti & Baldwin determined the relative amplitudes of the sinusoidal terms involving the k roots in order to form a complete solution for the problems of a semi-infinite radiating gas bounded by a wall undergoing sinusoidal oscillations in position and temperature. Baldwin (1962) superposed spatially damped sinusoidal waves to calculate the effect of radiative transfer on the propagation of an acoustic disturbance produced by impulsive wall motion. This problem was also studied by Lick (1964) and Moore (1966). The disturbance produced by a step input of wall radiation was also discussed by Baldwin (1962), further work being carried out by Solan & Cohen (1966) and by Cogley & Vincenti (1969).

More recently, Olfe & DePlomb (1970) carried out the solution for the decay of sinusoidal perturbations in an infinite radiating gas by determining the relative amplitudes of the sinusoidal terms involving the ω roots. They superposed temporally damped sinusoidal waves to calculate the decay of initial step temperature profiles consisting of constant temperature perturbations inside finite planar, cylindrical and spherical regions, with zero initial temperature perturbations outside.

Since at high temperatures a gas is likely to be ionized or partially ionized, electromagnetic effects may also be significant. Thus, the study of interaction of radiative and electromagnetic effects, such as may arise in problems of the solar photosphere, rocket re-entry, etc., is important. Helliwell & Nye (1969) studied the propagation of small amplitude waves, generated by small sinusoidal variations in the position and temperature of the plane bounding wall, in a semi-infinite expanse of a radiating gas of perfect electrical conductivity. Nye (1970*a*) carried out further work by extending the work of Helliwell & Nye to a radiating gas of finite but high electrical conductivity. Nye (1970*b*) also studied the linear problem of a piston impulsively started and moving into an electrically conducting, radiating gas, which is an extension of the work of Lick (1964) to the MGD regime.

The present study is an extension of the work of Olfe & DePlomb (1970) to the magnetogasdynamic regime. In §4 of this paper, we analyse the decay of sinusoidal perturbations in an infinite, thermally radiating gas of perfect electrical conductivity in the presence of a magnetic field. We determine the relative amplitudes of the sinusoidal terms involving the ω roots of the appropriate characteristic equation. In §§ 5 and 6, we consider the superposition of temporally damped sinusoidal waves to calculate the decay of initial step temperature profiles consisting of a constant temperature perturbation inside a finite planar region, with zero initial temperature perturbation outside. We carry out specific calculations taking the initial pressure and gas velocity perturbations to be zero. The pure sinusoidal case is a special self-similar case which depends on the parameters Γ (the radiation parameter) and B^2 (the magnetic interaction parameter). The superposed profiles are influenced by an additional parameter, namely the optical depth of the initial profile.

For a broad range of small and intermediate values of the Boltzmann number, the cooling proceeds in time from being a constant-density process to being a constant-pressure process. The magnetic field causes slower temperature decay with time and makes the step temperature profiles tend to approach constant-pressure cooling values. In contrast with slower temperature decay, the magnetic field causes faster decay of velocity and pressure perturbations. The magnetic field hastens the transition from constant-density cooling to constant-pressure cooling. This transition is produced by the magneto-acoustic waves generated near the profile edges by the radiative cooling.

2. Basic equations

A system of Cartesian axes is chosen so that the magnetic field H^* is parallel to the z axis. The electric field E^* and the current J^* are then parallel to the y axis. The fundamental equations governing the gas flow in the direction of the x axis may then be written down in conventional form using rationalized mks units. For simplicity the electrical conductivity of the gas is taken to be infinite and the effects of viscosity and thermal conductivity are neglected. The contributions from radiative scattering, radiative pressure and radiative energy density are also neglected. The effects of radiation enter only in the energy equation, which is

$$\rho^*\left(\frac{\partial \epsilon^*}{\partial t}+v^*\frac{\partial \epsilon^*}{\partial x}\right)=-p^*\frac{\partial v^*}{\partial x}+Q_r^*. \tag{1}$$

Here, ϵ^* is the specific internal energy of the gas, defined by the equations of state

$$\epsilon^* = RT^*/(\gamma-1), \quad p^* = R\rho^*T^*, \tag{2}$$

where p^*, ρ^*, T^* and v^* are the pressure, density, temperature and velocity respectively; R and γ are the gas constant and the ratio of specific heats, respectively. The quantity Q_r^* expresses the contribution to the heat transfer from the radiative flux. As is well known (see, for example, Kourganoff 1952) Q_r^* may be expressed in terms of certain integrals. In order to pursue the analysis an approximation must be made which removes these integrals (see Helliwell 1966). We shall adopt here the Milne–Eddington approximation. Then Q_r^* is given by

$$Q_r^* = \alpha^*(G^*-4\pi B^*), \tag{3}$$

where G^* satisfies the equation

$$(\tfrac{1}{3}\partial^2/\partial\bar{z}^2-1)\,G^* = -4\pi B^*. \tag{4}$$

Here, $B^* = \tilde{\sigma}T^{*4}/\pi$, $\tilde{\sigma}$ is the Stefan's constant, α^* is the absorption coefficient and the co-ordinate $\bar{z}$ is defined by the differential relation $d\bar{z} = \alpha^*\,dx$. The rest of the equations of motion (with the electrical conductivity of the gas infinite) are

$$\partial E^*/\partial x = -\mu\,\partial H^*/\partial t, \tag{5}$$

$$E^* = \mu H^* v^*, \tag{6}$$

$$\partial\rho^*/\partial t+\partial(\rho^*v^*)/\partial x = 0, \tag{7}$$

$$\rho^*\left(\frac{\partial v^*}{\partial t}+v^*\frac{\partial v^*}{\partial x}\right)=-\frac{\partial}{\partial x}(p^*+\tfrac{1}{2}\mu H^{*2}), \tag{8}$$

where μ is the magnetic permeability.

3. Linearized equations

We now linearize the foregoing equations in the usual manner by setting $v^* = v$, $p^* = p_0+p$, $H^* = H_0+H$, $G^* = G_0+G$ and so on. Here the quantities with suffix 0 denote values in the uniform state and the unstarred quantities are

small. The constant $G_0 = 4\tilde{\sigma}T_0^4$ is a measure of the rate of emission of radiation energy from any point in the gas in the uniform state. On carrying out the process of linearization, the equations governing the gas flow become

$$\partial E/\partial x = -\mu(\partial H/\partial t), \tag{9}$$

$$E = \mu H_0 v, \tag{10}$$

$$\partial\rho/\partial t + \rho_0(\partial v/\partial x) = 0, \tag{11}$$

$$\rho_0(\partial v/\partial t) = -\partial(p + \mu H_0 H)/\partial x, \tag{12}$$

$$\rho_0 \frac{\partial}{\partial t}\left(\frac{RT}{\gamma - 1}\right) = -p_0 \frac{\partial v}{\partial x} + \alpha_0(G - 4G_0 T/T_0), \tag{13}$$

$$\left(\frac{1}{3\alpha_0^2}\frac{\partial^2}{\partial x^2} - 1\right) G = -4G_0(T/T_0), \tag{14}$$

$$p/p_0 = \rho/\rho_0 + T/T_0, \tag{15}$$

where α_0 is the linear absorption coefficient evaluated at the uniform condition T_0 and ρ_0. The introduction of a potential function ϕ such that

$$v = \partial\phi/\partial x, \quad p + \mu H_0 H = -\rho_0 \partial\phi/\partial t \tag{16}$$

ensures that the momentum equation (12) is satisfied. It is easy to show that

$$\frac{\partial}{\partial t}\left(\frac{p}{p_0}\right) = -\frac{1}{a_T^2}\left(\frac{\partial^2}{\partial t^2} - A^2\frac{\partial^2}{\partial x^2}\right)\phi, \tag{17}$$

where a_T and A are the isothermal sound speed and Alfvén wave speed respectively and are given by

$$a_T^2 = p_0/\rho_0, \quad A^2 = \mu H_0^2/\rho_0.$$

By elimination between the above equations, it can be shown that ϕ satisfies the equation

$$\left[\frac{\partial^3}{\partial t\,\partial x^2}\left(\frac{1}{c_s^2}\frac{\partial^2}{\partial t^2} - \frac{\partial^2}{\partial x^2}\right) + \frac{16a_0\gamma}{Bo}\alpha_0\frac{c_T^2}{c_s^2}\frac{\partial^2}{\partial x^2}\left(\frac{1}{c_T^2}\frac{\partial^2}{\partial t^2} - \frac{\partial^2}{\partial x^2}\right) - 3\alpha_0^2\frac{\partial}{\partial t}\left(\frac{1}{c_s^2}\frac{\partial^2}{\partial t^2} - \frac{\partial^2}{\partial x^2}\right)\right]\phi = 0, \tag{18}$$

where $c_s^2 = a_0^2 + A^2$, $c_T^2 = a_0^2/\gamma + A^2$ and Bo represents the Boltzmann number, a dimensionless convection–radiation parameter defined by

$$Bo = R\gamma\rho_0 a_0/(\gamma - 1)\,\tilde{\sigma}T_0^3.$$

Here, a_0 is the acoustic speed, given by $a_0^2 = \gamma p_0/\rho_0$, and c_s and c_T are the magneto-acoustic speed and magneto-isothermal speed, which are the generalizations of the acoustic speed and isothermal speed.

4. Sinusoidal perturbations

Substitution of a sinusoidal perturbation $\phi \propto \exp[i(\omega t - kx)]$ into (18) gives a characteristic equation, which may be solved for either ω or k. The characteristic equation is a cubic in terms of ω and a quadratic in k^2. For the spatially damped problem treated by Helliwell & Nye (1969), ω is fixed because the magneto-acoustic waves are generated at a wall which is oscillating in position and temperature at the fixed frequency ω. Expressed in terms of the dimensionless complex wave speed $\chi = -(ic_s/\omega)k$, the quadratic characteristic equation for χ^2 yields the unequal roots χ_1^2 and χ_2^2. There occur two types of disturbances, corresponding to χ_1 and χ_2. One of them is essentially a magneto-acoustic wave and the other is a radiation-induced wave.

For the decay problem treated in this section, k is fixed. It is convenient to work with the non-dimensional frequency $\sigma = \omega/ika_0$ and a propagation vector $\mathbf{k}$ in the direction of the initial sinusoidal disturbance. Substitution of

$$\phi \propto \exp(-\sigma k a_0 t + i\mathbf{k}.\mathbf{s})$$

into (18) provides the following characteristic equation for σ:

$$\sigma^3 - \Gamma\gamma\sigma^2 + (1+B^2)\sigma - \Gamma\xi = 0, \quad \xi = (1+B^2\gamma), \tag{19}$$

where $B^2 = A^2/a_0^2$, a non-dimensional magnetic interaction parameter. The non-dimensional radiation parameter Γ is given by

$$\Gamma_{\text{approx}} = \left(\frac{16}{Bo}\right)\left(\frac{Bu}{1+3Bu^2}\right), \tag{20}$$

the subscript 'approx' signifying that the differential approximation has been used. The Bouguer number $Bu = \alpha_0/k = \alpha_0\lambda/2\pi$ is a dimensionless parameter which measures the opacity of the gas enclosed within a wavelength λ of the sinusoidal disturbance.

For a grey gas the exact expression for Γ (see Olfe & DePlomb 1970) is

$$\begin{aligned}\Gamma &= (16/Bo)\,Bu[1 - Bu\tan^{-1}Bu^{-1}] \\ &= (16/Bo)\,\kappa[1 - \kappa\tan^{-1}\kappa^{-1}],\end{aligned} \tag{21}$$

where $\kappa = 1/Bu$ is a non-dimensional wavenumber for the sinusoidal disturbance.

In this temporally damped case the Boltzmann number Bo and Bouguer number Bu are combined into a single radiation parameter Γ. This result was produced by the choice of sinusoidal profile for the initial disturbance. For a sinusoidal profile the energy absorbed at a point, as well as the energy emitted, is proportional to the local temperature perturbation at the point (see, for example, Smith 1957; Golitsyn 1963). Therefore the decaying disturbance retains sinusoidal shape and a change in Bu is equivalent to the corresponding change in Bo which produces the same net radiation.

Let us now examine the roots of (19). The coefficients of the σ terms are such that there is one real root σ_0 and a pair of complex conjugate roots $\sigma_\pm = \sigma_r \pm i\sigma_i$,

where σ_r and σ_i are real. In the limits of small and large values of the radiation parameter Γ the following values are obtained:

$$\left.\begin{aligned} &\sigma_0 \to \frac{\Gamma\xi}{1+B^2} = \delta_0, \quad \sigma_r \to \frac{\gamma-1}{2\Gamma(1+B^2)} = \delta_r, \quad \sigma_i \to (1+B^2)^{\frac{1}{2}} = \delta_i \quad \text{for} \quad \Gamma \ll 1, \\ &\sigma_0 \to \Gamma\gamma = \delta_0', \quad \sigma_r \to \frac{\gamma-1}{2\Gamma\gamma^2} = \delta_r^1, \quad \sigma_i \to \left(\frac{\xi}{\gamma}\right)^{\frac{1}{2}} = \delta_i' \quad \text{for} \quad \Gamma \gg 1. \end{aligned}\right\} \tag{22}$$

The roots σ_0, σ_r and σ_i vary smoothly between the above limits for all values of B^2 as shown in figure 1 for $\gamma = \frac{5}{3}$.

We shall proceed to calculate the amplitudes of the terms involving the three decay frequencies, i.e. we shall carry out the complete solution for the decay of initial sinusoidal perturbations in temperature, velocity and pressure.

The total solution for the decay of sinusoidal perturbations consists of the three exponential terms involving the three decay frequencies σ_0, σ_+ and σ_-, respectively. Accordingly, the solution for the potential ϕ is given by

$$\phi = \mathrm{Re}\,[(a_0/k)\,(c_0 e^{-\sigma_0 k a_0 t} + c_+ e^{-\sigma_+ k a_0 t} + c_- e^{-\sigma_- k a_0 t})\, e^{i\mathbf{k}.\mathbf{s}}], \tag{23}$$

where Re denotes the real part. The complex non-dimensional amplitudes c_0 and $c_\pm$ are determined below in terms of the parameters Γ and B^2 and initial conditions. Substitution of (23) into (16) and (17) yields the relations for the perturbation velocity v and the perturbation pressure p. The relation for the perturbation temperature T can be obtained by substituting (23) in

$$\frac{\partial}{\partial t}\left(\frac{T}{T_0}\right) = \left[(1+B^2\gamma)\frac{\partial^2}{\partial x^2} - \frac{\gamma}{a_0^2}\frac{\partial^2}{\partial t^2}\right]\phi.$$

Thus, the relations for the perturbation velocity v in the $\mathbf{k}$ direction and the perturbation pressure p and temperature T are

$$v/a_0 = \mathrm{Re}\,[i(c_0 e^{-\sigma_0 k a_0 t} + c_+ e^{-\sigma_+ k a_0 t} + c_- e^{-\sigma_- k a_0 t})\, e^{i\mathbf{k}.\mathbf{s}}], \tag{24}$$

$$p/p_0 = \mathrm{Re}\,[\{\gamma_0 e^{-\sigma_0 k a_0 t} + \gamma_+ e^{-\sigma_+ k a_0 t} + \gamma_- e^{-\sigma_- k a_0 t}\}\, e^{i\mathbf{k}.\mathbf{s}}], \tag{25}$$

$$T/T_0 = \mathrm{Re}\,[\{b_0 e^{-\sigma_0 k a_0 t} + b_+ e^{-\sigma_+ k a_0 t} + b_- e^{-\sigma_- k a_0 t}\}\, e^{i\mathbf{k}.\mathbf{s}}], \tag{26}$$

where the amplitudes γ_0, $\gamma_\pm$, b_0 and $b_\pm$ are related to c_0 and $c_\pm$ by

$$\left.\begin{aligned} \gamma_0 &= \gamma(\sigma_0 + B^2/\sigma_0)c_0, \quad \gamma_\pm = \gamma(\sigma_\pm + B^2/\sigma_\pm)c_\pm, \\ b_0 &= (\gamma\sigma_0 + \xi/\sigma_0)c_0, \quad b_\pm = \gamma(\gamma\sigma_\pm + \xi/\sigma_\pm)c_\pm. \end{aligned}\right\} \tag{27}$$

For the initial conditions we consider the following sinusoidal disturbances:

$$\left.\begin{aligned} T(\mathbf{s},0) &= \mathrm{Re}\,[(b_0+b_++b_-)\, e^{i\mathbf{k}.\mathbf{s}}] = \mathrm{Re}\,[\Delta_1 e^{i\mathbf{k}.\mathbf{s}}], \\ v(\mathbf{s},0)/a_0 &= \mathrm{Re}\,[i(c_0+c_++c_-)\, e^{i\mathbf{k}.\mathbf{s}}] = \mathrm{Re}\,[\Delta_2 e^{i\mathbf{k}.\mathbf{s}}], \\ p(\mathbf{s},0)/p_0 &= \mathrm{Re}\,[(\gamma_0+\gamma_++\gamma_-)\, e^{i\mathbf{k}.\mathbf{s}}] = \mathrm{Re}\,[\Delta_3 e^{i\mathbf{k}.\mathbf{s}}], \end{aligned}\right\} \tag{28}$$

where the amplitudes Δ_j may be complex to allow for arbitrary phase differences between initial sinusoidal disturbances. Equations (27) and (28) may be solved for the perturbation amplitudes, expressed in terms of the roots σ_0, σ_r and σ_i.

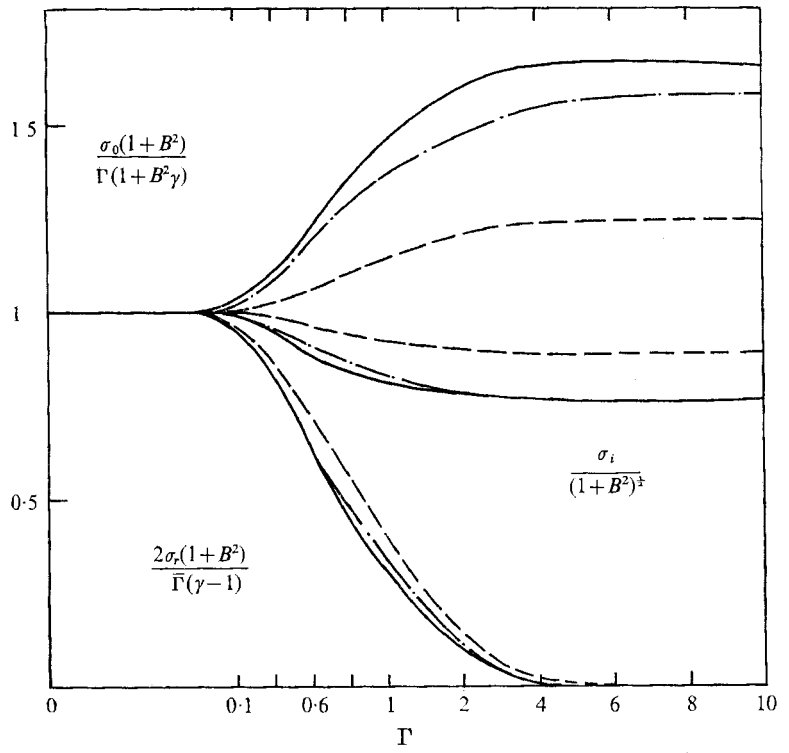

FIGURE 1. Real and imaginary decay frequencies against Γ; $\gamma = \frac{5}{3}$. ——, $B^2 = 0$; —·—, $B^2 = 0{\cdot}1$; – – –, $B^2 = 1$.

We find

$$c_0 = (\gamma\sigma_0 + \xi/\sigma_0)^{-1} b_0$$
$$= \frac{[\sigma_r^2+\sigma_i^2-B^2]\Delta_1 + 2i\sigma_r\Delta_2 + \Delta_3[\xi-(\sigma_r^2+\sigma_i^2)]\gamma^{-1}}{\sigma_0^{-1}(\sigma_r^2+\sigma_i^2)+\sigma_0-2\sigma_r}, \tag{29a}$$

$$c_\pm = \pm C - Dc_0, \quad C = C_1 + C_2, \quad D = D_1 + D_2, \tag{29b}$$

$$C_1 = \frac{1}{2\sigma_i}\frac{\Delta_2}{\sigma_r^2+\sigma_i^2-B^2}[(\sigma_r^2+\sigma_i^2)(\sigma_r \mp i\sigma_i) + B^2(\sigma_r \pm i\sigma_i)], \tag{29c}$$

$$C_2 = -i\Delta_3\gamma^{-1}(\sigma_r^2+\sigma_i^2)/2\sigma_i(\sigma_r^2+\sigma_i^2-B^2), \tag{29d}$$

$$D_1 = \frac{\sigma_r^2+\sigma_i^2}{2(\sigma_r^2+\sigma_i^2-B^2)}\left[1 \pm i\frac{\sigma_r-\sigma_0}{\sigma_i}\right], \tag{29e}$$

$$D_2 = -\frac{B^2}{2(\sigma_r^2+\sigma_i^2-B^2)}\left[1 \pm i\frac{\sigma_r^2+\sigma_i^2-\sigma_0\sigma_r}{\sigma_0\sigma_i}\right], \tag{29f}$$

$$\frac{b_\pm}{b_0} = \frac{1}{(\gamma\sigma_0+\xi/\sigma_0)(\sigma_r^2+\sigma_i^2)}[\{\xi+\gamma(\sigma_r^2+\sigma_i^2)\}\sigma_r \mp \{\xi-\gamma(\sigma_r^2+\sigma_i^2)\}\sigma_i]\frac{c_0}{c_\pm}. \tag{29g}$$

The relative decay of sinusoidal disturbances is thus given by (24), (25), (26) and (29*a–g*) expressed in terms of the roots σ_0, σ_r and σ_i, which may be determined

from the cubic equation (19) for any value of the radiation parameter Γ and the magnetic parameter B^2. For the limiting values of σ_0, σ_r and σ_i given in (22), the following solutions are obtained.

For $\Gamma \ll 1$,

$$\frac{T}{T_0} \to \mathrm{Re}\left\{\left[\left(\frac{\xi}{1+B^2}(\Delta_1+\Delta_3\gamma^{-1}-\Delta_3)\right)e^{-\delta_0 k a_0 t}\right.\right.$$
$$+\left(\frac{(1-\gamma)B^2}{1+B^2}(\Delta_1+\Delta_3\gamma^{-1}-\Delta_3)\cos(\delta_i k a_0 t) - i\frac{\gamma-1}{(1+B^2)^{\frac{1}{2}}}\sin(\delta_i k a_0 t)\right.$$
$$\left.\left.+(1-\gamma^{-1})\Delta_3\cos(\delta_i k a_0 t)\right)e^{-\delta_r k a_0 t}\right] e^{i\mathbf{k}.\mathbf{s}}\Big\}, \tag{30a}$$

$$\frac{v}{a_0} \to \mathrm{Re}\left\{\left[\left(\frac{B^2 i}{(1+B^2)^{\frac{1}{2}}}(\Delta_1+\Delta_3\gamma^{-1}-\Delta_3)\sin(\delta_i k a_0 t)+\Delta_2\cos(\delta_i k a_0 t)\right.\right.$$
$$\left.\left.-i\Delta_3\gamma^{-1}(1+B^2)^{\frac{1}{2}}\sin(\delta_i k a_0 t)\right)e^{-\delta_r k a_0 t}\right] e^{i\mathbf{k}.\mathbf{s}}\Big\}, \tag{30b}$$

$$\frac{p}{p_0} \to \mathrm{Re}\left\{\left[\frac{B^2}{1+B^2}(\Delta_1+\Delta_3\gamma^{-1}-\Delta_3)e^{-\delta_0 k a_0 t}+\left(-\frac{\gamma B^2}{1+B^2}(\Delta_1+\Delta_3\gamma^{-1}-\Delta_3)\cos(\delta_i k a_0 t)\right.\right.\right.$$
$$\left.\left.\left.-\frac{i\gamma\Delta_2}{(1+B^2)^{\frac{1}{2}}}\sin(\delta_i k a_0 t)+\Delta_3\cos(\delta_i k a_0 t)\right)e^{-\delta_r k a_0 t}\right] e^{i\mathbf{k}.\mathbf{s}}\Big\}. \tag{30c}$$

For $\Gamma \gg 1$,

$$T/T_0 \to \mathrm{Re}\left[\Delta_1 e^{-\delta_0' k a_0 t} e^{i\mathbf{k}.\mathbf{s}}\right], \tag{31a}$$

$$\frac{v}{a_0} \to \mathrm{Re}\left\{\left[\left(i(\Delta_1-\Delta_3)\left(\frac{\xi}{\gamma}\right)^{\frac{1}{2}}\sin(\delta_i' k a_0 t)+\Delta_2\cos(\delta_i' k a_0 t)\right)e^{-\delta_r' k a_0 t}\right] e^{i\mathbf{k}.\mathbf{s}}\right\}, \tag{31b}$$

$$\frac{p}{p_0} \to \mathrm{Re}\left\{\left[\Delta_1\exp(-\delta_0' k a_0 t)+\{(\Delta_3-\Delta_1)\cos(\delta_i' k a_0 t)\right.\right.$$
$$\left.\left.-i\Delta_2(\gamma/\xi)^{\frac{1}{2}}\sin(\delta_i' k a_0 t)\}e^{-\delta_r' k a_0 t}\right] e^{i\mathbf{k}.\mathbf{s}}\right\}. \tag{31c}$$

In (30) and (31) the omitted terms are $\Gamma\Delta_j$ and Δ_j/Γ. For the case of no initial velocity or pressure perturbations (30) and (31) represent constant-pressure and constant-density cooling, respectively.

The constant-density solution (31) is to be expected since the gas does not have time to move during the cooling period for a sufficiently large cooling rate. The cooling time given by (31) is of order $1/\Gamma$, which is much shorter than the period of velocity and pressure oscillations. The period of these oscillations becomes comparable, for sufficiently large values of B^2, with the cooling time.

We observe that (30) gives a cooling time of order $1/\Gamma$, which is much longer than the period of velocity and pressure oscillations. In the presence of the magnetic field, an initial temperature profile of amplitude Δ_1 induces velocity and pressure perturbations of order Δ_1. These induced pressures and velocities are negligible in the non-conducting case. In the present case the period of oscillations of velocity and pressure decreases as the magnetic field parameter B^2 is increased.

For planetary atmospheres Γ is much less than unity. On the other hand Γ can be of order unity in stellar atmospheres. Also, engineering applications or

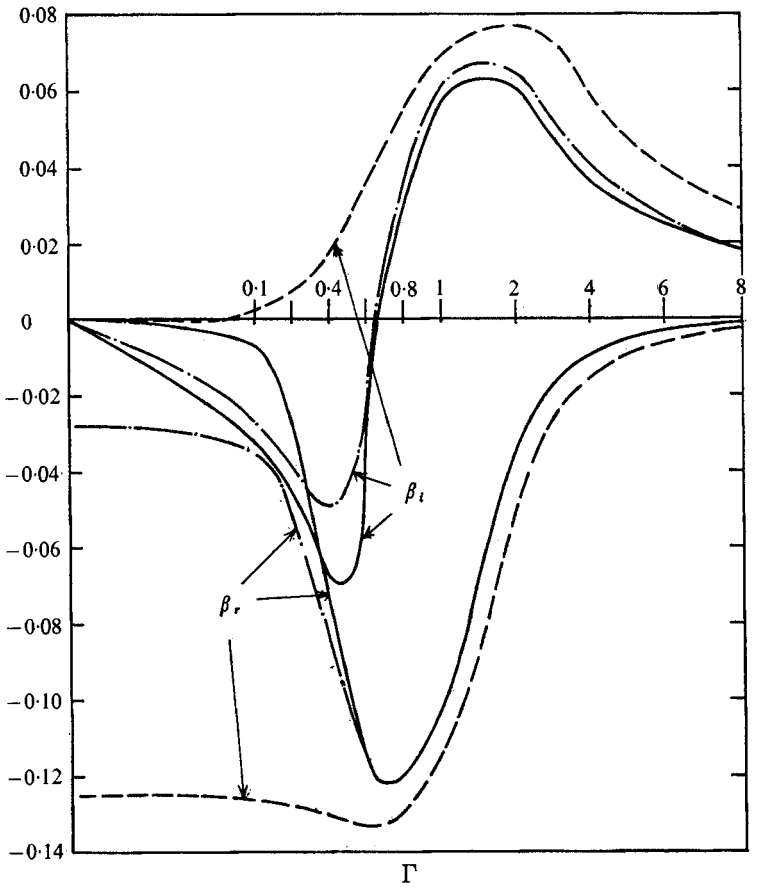

FIGURE 2. Temperature decay coefficients against Γ; $\gamma = \frac{5}{3}$.
——, $B^2 = 0$; —·—, $B^2 = 0{\cdot}1$; – – –, $B^2 = 1$.

laboratory experiments can involve high temperatures with corresponding Γ values up to unity or greater. For intermediate values of Γ all three roots σ_0, σ_+ and σ_- will contribute to the temperature cooling. If an initial perturbation only in the temperature is considered the amplitude b_0 is given by (29*a*) with $\Delta_2 = \Delta_3 = 0$ and the relative amplitudes of the terms containing $\sigma_\pm$ are given by

$$b_\pm/b_0 = \beta_r \pm i\beta_i, \tag{32}$$

$$\left.\begin{aligned}\beta_r &= \frac{1}{\gamma\sigma_0+\xi/\sigma_0}\frac{1}{\sigma_r^2+\sigma_i^2}[\gamma_r\sigma_r\{\xi+\gamma(\sigma_r^2+\sigma_i^2)\}+\gamma_i\sigma_i\{\xi-\gamma(\sigma_r^2+\sigma_i^2)\}],\\ \beta_i &= \frac{1}{\gamma\sigma_0+\xi/\sigma_0}\frac{1}{\sigma_r^2+\sigma_i^2}[\gamma_i\sigma_r\{\xi+\gamma(\sigma_r^2+\sigma_i^2)\}-\gamma_r\sigma_i\{\xi-\gamma(\sigma_r^2+\sigma_i^2)\}],\end{aligned}\right\} \tag{33}$$

where
$$\left.\begin{aligned}&c_\pm = \gamma_r \pm i\gamma_i, \quad \gamma_r = -\tfrac{1}{2},\\ &\gamma_i = -\frac{1}{2}\frac{1}{\sigma_r^2+\sigma_i^2-B^2}\left[\frac{(\sigma_r^2+\sigma_i^2)(\sigma_r-\sigma_0)}{\sigma_i}-B^2\left\{\frac{\sigma_r^2+\sigma_i^2-\sigma_0\sigma_r}{\sigma_0\sigma_i}\right\}\right].\end{aligned}\right\} \tag{34}$$

The temperature decay coefficients β_r and β_i as functions of the radiation parameter Γ for $B^2 = 0$, 0·1 and 1 are plotted in figure 2 with $\gamma = \frac{5}{3}$. We notice in particular the behaviour of β_r and β_i in the ranges $\Gamma \ll 1$ and $\Gamma \gg 1$. If $B^2 = 0$, β_r, $\beta_i \to 0$ in these ranges. If $B^2 \neq 0$, β_r and β_i deviate from zero, and the deviation increases with increasing B^2.

For b_0 real the solutions (24)–(26) reduce to

$$\left.\begin{aligned} T/T_0 &= b_0[e^{-\sigma_0 k a_0 t} + 2e^{-\sigma_r k a_0 t}\{\beta_r \cos(\sigma_i k a_0 t) + \beta_i \sin(\sigma_i k a_0 t)\}] \cos(\mathbf{k}.\mathbf{s}), \\ v/a_0 &= -c_0[e^{-\sigma_0 k a_0 t} + 2e^{-\sigma_r k a_0 t}\{\gamma_r \cos(\sigma_i k a_0 t) + \gamma_i \sin(\sigma_i k a_0 t)\}] \sin(\mathbf{k}.\mathbf{s}), \\ p/p_0 &= \gamma_0[e^{-\sigma_0 k a_0 t} + 2e^{-\sigma_r k a_0 t}\{\lambda_r \cos(\sigma_i k a_0 t) + \lambda_i \sin(\sigma_i k a_0 t)\}] \cos(\mathbf{k}.\mathbf{s}), \end{aligned}\right\} \quad (35)$$

where

$$\gamma_\pm/\gamma_0 = \lambda_r \pm i\lambda_i,$$

$$\lambda_r = \frac{1}{\sigma_0 + B^2/\sigma_0} \frac{1}{\sigma_r^2 + \sigma_i^2}[(\gamma_r\sigma_r + \gamma_i\sigma_i)(\sigma_r^2 - \sigma_i^2 + B^2) - 2(\sigma_r\gamma_i - \sigma_i\gamma_r)\sigma_r\sigma_i],$$

$$\lambda_i = \frac{1}{\sigma_0 + B^2/\sigma_0} \frac{1}{\sigma_r^2 + \sigma_i^2}[2\sigma_r\sigma_i(\gamma_r\sigma_r + \gamma_i\sigma_i) + (\gamma_i\sigma_r - \sigma_i\gamma_r)(\sigma_r^2 - \sigma_i^2 + B^2)].$$

5. Radiative decay of planar step temperature profiles

The sinusoidal perturbations of §4 may be superposed to yield solutions for the decay of any initial temperature, velocity and pressure profiles in a radiating gas. In this section we obtain a solution for the decay of planar step temperature profiles.

Consider the decay of a planar step temperature profile, i.e. an initial temperature perturbation which has the constant value $T_0\Delta$ between $\pm x_0$ and is zero elsewhere. Superposition of the solutions (35) with $\mathbf{k}.\mathbf{s} = kx$ gives

$$\left.\begin{aligned} \frac{T(x,t)}{T_0} &= \int_0^\infty \bar{T}(k,t)\cos(kx)\,dk, \\ \frac{v(x,t)}{a_0} &= \int_0^\infty \bar{v}(k,t)\sin(kx)\,dk, \\ \frac{p(x,t)}{p_0} &= \int_0^\infty \bar{p}(k,t)\cos(kx)\,dk, \end{aligned}\right\} \quad (36)$$

with $\bar{T}(k,t)$, $\bar{v}(k,t)$ and $\bar{p}(k,t)$ corresponding to the right-hand sides of (35) without the $\mathbf{k}.\mathbf{s}$ factors. At the initial time $\bar{T}(k,0) = b_0(1+2\beta_r)$. Application of Fourier cosine transform theory to the initial temperature profile yields the following expression for $b_0(k)$:

$$\begin{aligned} b_0(k) &= (1+2\beta_r)^{-1}\bar{T}(k,0) = (1+2\beta_r)^{-1}\frac{2}{\pi}\int_0^\infty \frac{T(x,0)}{T_0}\cos(kx)\,dx \\ &= \frac{2\Delta\sin(kx_0)}{\pi k(1+2\beta_r)}. \end{aligned} \quad (37)$$

Substitution of $b_0(k)$ into (35) gives the following solutions expressed in terms of the non-dimensional time $\tau = \alpha_0 a_0 t$ and optical distances $\eta = \alpha_0 x$ and $\eta_0 = \alpha_0 x_0$:

$$\frac{T(\eta,\tau)}{T_0\Delta} = \frac{2}{\pi}\int_0^\infty [e^{-\sigma_0\kappa\tau} + 2e^{-\sigma_0\kappa\tau}\{\beta_r\cos(\sigma_i\kappa\tau) + \beta_i\sin(\sigma_i\kappa\tau)\}] \frac{\cos(\kappa\eta)\sin(\kappa\eta_0)}{(1+2\beta_r)\kappa}\,d\kappa, \quad (38)$$

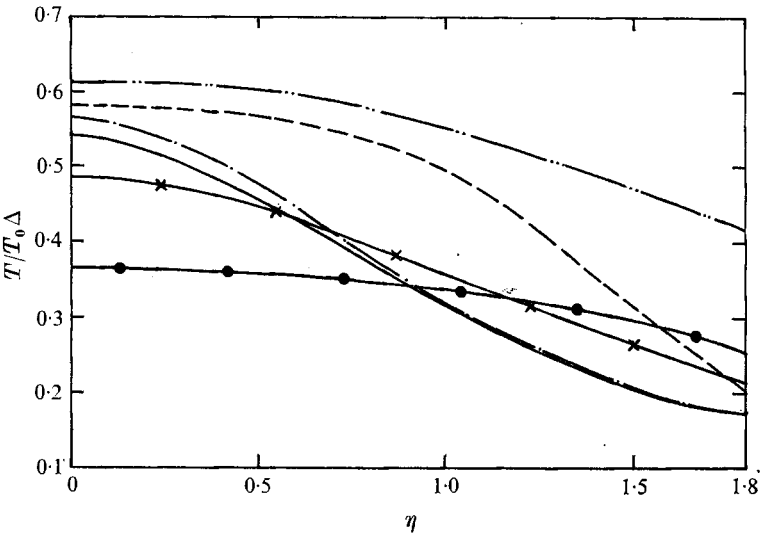

FIGURE 3. Temperature perturbation profiles, for $2\eta_0 = 2$, $\gamma = \frac{5}{3}$, $Bo = 5$. $\bar{\tau} = 5$: —, $B^2 = 0$; —·—, $B^2 = 0{\cdot}1$; — — —, $B^2 = 1$; —··—, $B^2 = 10$. $\bar{\tau} = 10$: —●—, $B^2 = 0$; —×—, $B^2 = 1$.

$$\frac{v(\eta,\tau)}{a_0\Delta} = -\frac{2}{\pi}\int_0^\infty [e^{-\sigma_0\kappa\tau} + 2e^{-\sigma_r\kappa\tau}\{\gamma_r\cos(\sigma_i\kappa\tau) + \gamma_i\sin(\sigma_i\kappa\tau)\}] \times \frac{\sin(\kappa\eta)\sin(\kappa\eta_0)}{(1+2\beta_r)\kappa}\frac{\sigma_0}{\gamma\sigma_0^2+\xi}d\kappa, \tag{39}$$

$$\frac{p(\eta,\tau)}{p_0\gamma\Delta} = \frac{2}{\pi}\int_0^\infty [e^{-\sigma_0\kappa\tau} + 2e^{-\sigma_r\kappa\tau}\{\lambda_r\cos(\sigma_i\kappa\tau) + \lambda_i\sin(\sigma_i\kappa\tau)\}] \times \frac{\cos(\kappa\eta)\sin(\kappa\eta_0)}{(1+2\beta_r)\kappa}\left(\sigma_0+\frac{B^2}{\sigma_0}\right)\frac{\sigma_0}{\gamma\sigma_0^2+\xi}d\kappa. \tag{40}$$

The factors β_r, β_i, γ_r, γ_i, λ_r and λ_i are all defined earlier and are determined from the cubic equation (19) involving the parameters Γ and B^2. For a grey gas Γ is given by (21). Equations (38)–(40) contain two independent parameters Bo and η_0. We introduce another non-dimensional time $\bar{\tau} = (16/Bo)\tau$ into (38)–(40) which is proportional to the amount of energy emitted up to time t. Reference to the integrals in (38)–(40) shows that we cannot combine Bo and η_0 into a single parameter because the component sinusoidal functions are weighted differently for different times and positions. As a result the profile shapes depend on the optical width of the initial step. Also, the step profiles decay through a series of non-similar profiles, i.e. the shapes of the profiles may vary with time. This is in contrast with the pure sinusoidal profiles, which retain their original shape.

6. Numerical solutions to the integrals and discussion

Numerical evaluation of the integral in (38) on a computer for a grey gas has provided the temperature perturbation profiles shown in figures 3–5. Figure 3 shows perturbation temperature profiles for the initial profile of optical thickness $2\eta_0 = 2$ for $Bo = 5$, $\bar{\tau} = 5$ and $B^2 = 0$, 0·1, 1 and 10. These profiles show that the

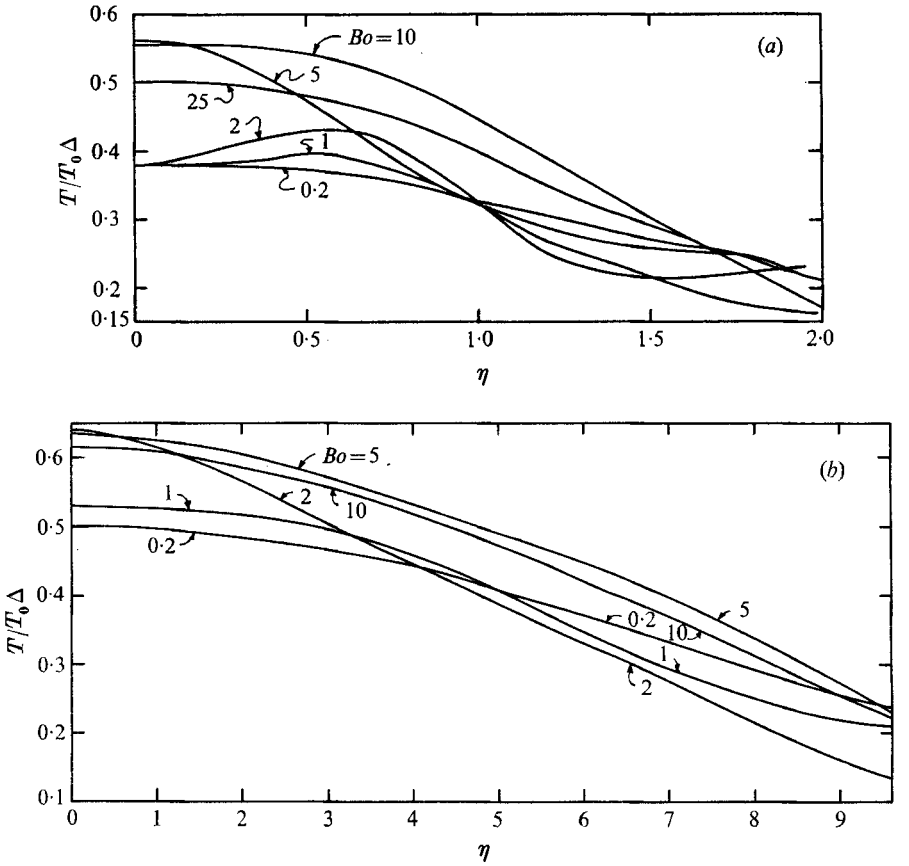

FIGURE 4. Temperature perturbation profiles: $\gamma = \frac{5}{3}$, $B^2 = 0{\cdot}1$, $Bo = 0{\cdot}2, 1, 2, 5, 10, 25$. (*a*) $2\eta_0 = 2, \bar{\tau} = 5$. (*b*) $2\eta_0 = 10, \bar{\tau} = 50$.

magnetic field keeps the gas hotter than the corresponding non-conducting gas. The stronger the magnetic field the hotter is the gas. We notice that the magnetic field causes slower temperature decay with time $\bar{\tau}$. This is clear from the profiles for $B^2 = 0$ and 1 at times $\bar{\tau} = 5$ and 10 shown in this figure. From the profiles for $B^2 = 0, 0{\cdot}1, 1$ and 10 at $\bar{\tau} = 5$ we note that the magnetic field makes the temperature perturbations tend to approach constant-pressure cooling values.

In figures 4 (*a*) and (*b*), we have shown perturbation temperature profiles for the profile widths $2\eta_0 = 2$ and 10, respectively. The temperature profiles are drawn for $Bo = 0{\cdot}2, 1, 2, 5, 10$ and 25 for $\bar{\tau} = 5$ in figure 4 (*a*). The transition from the constant-pressure cooling to constant-density cooling can be noticed from the profiles for $Bo = 25$ and $0{\cdot}2$ in figure 4 (*a*), i.e. for large and small Bo values. A gas characterized by intermediate Bo values will progress in time from constant-density cooling to constant-pressure cooling. We have shown the profiles for $Bo = 0{\cdot}2, 1, 2, 5$ and 10 at $\bar{\tau} = 50$ in figure 4 (*b*). Comparison of figures 4 (*a*) and (*b*) shows that increased absorption results in a slower temperature decay with time $\bar{\tau}$. The profiles become more continuous as the gas in the region $\eta > \eta_0$ gets heated as time progresses (see figure 4 (*b*)).

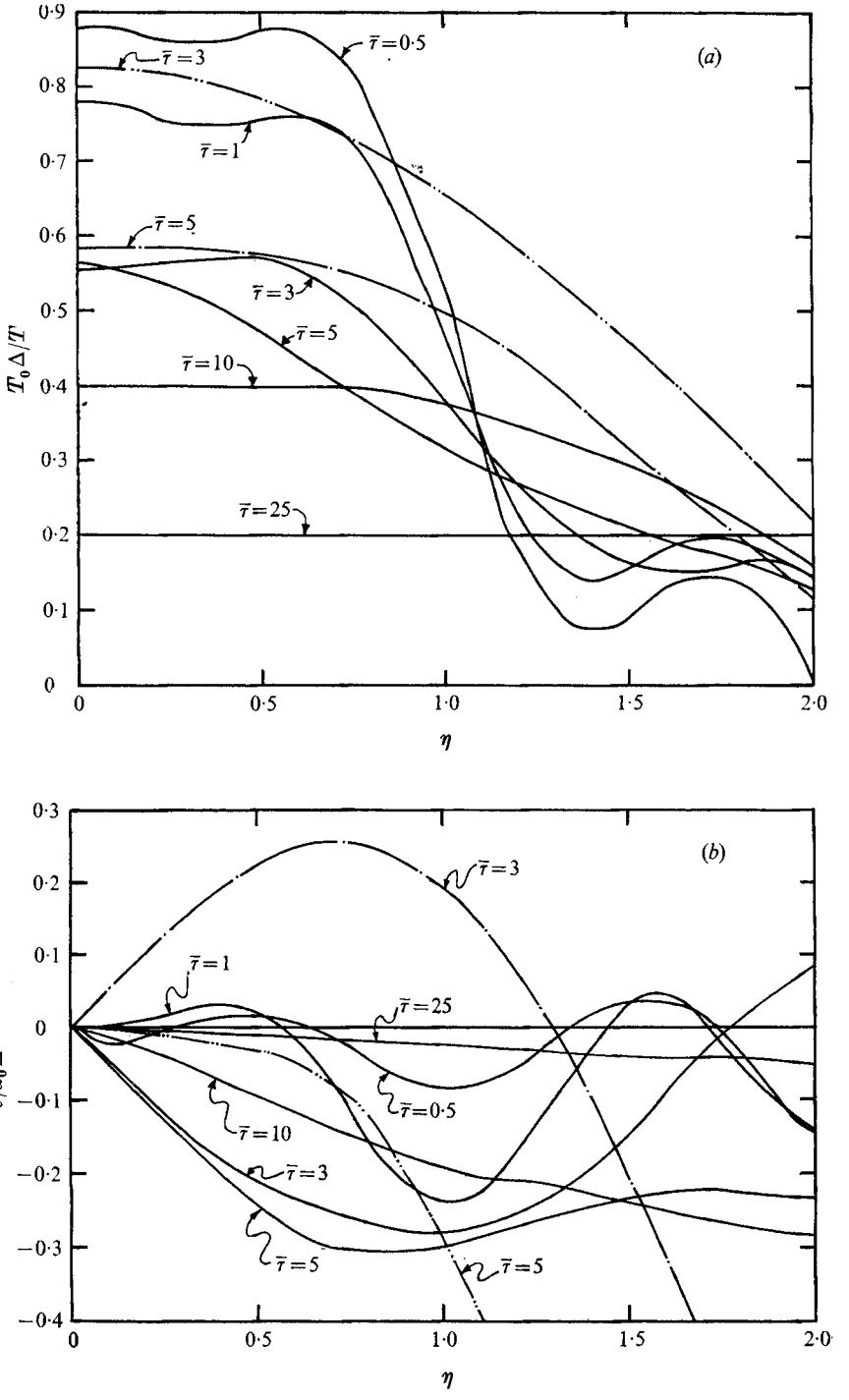

FIGURES 5(*a*) and (*b*). For legend see following page.

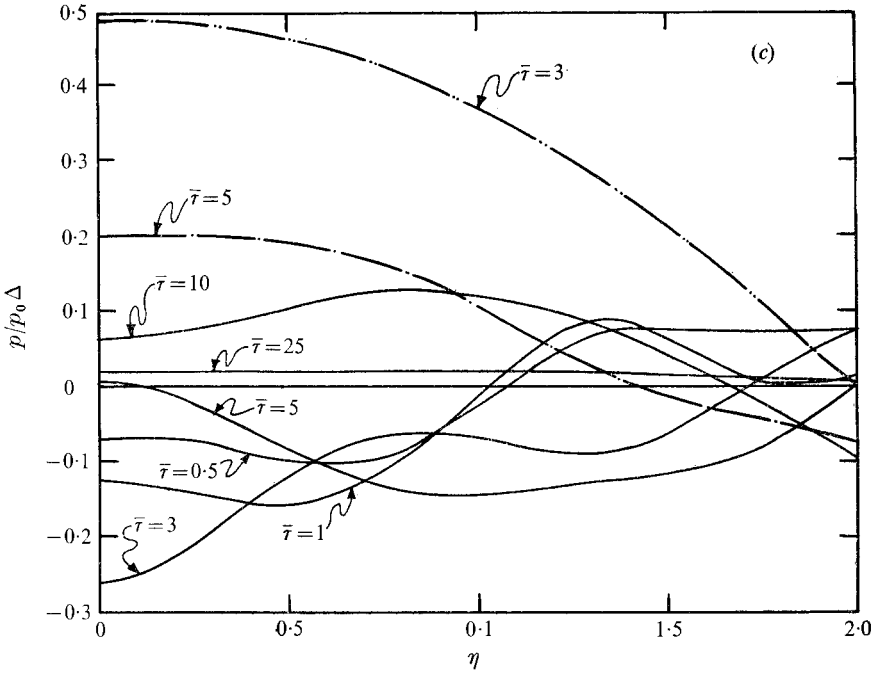

FIGURE 5. (*a*) Temperature, (*b*) velocity and (*c*) pressure perturbation profiles: $2\eta_0 = 2$, $\gamma = \frac{5}{3}$, $Bo = 5$. ——, $B^2 = 0{\cdot}1$; —·—, $B^2 = 1$; —··—, $B^2 = 10$.

Decay features for intermediate Boltzmann numbers

The integrals appearing in (38)–(40) are evaluated for an intermediate Boltzmann number $Bo = 5$ and $\eta_0 = 1$. Figure 5 (*a*) shows the decay of initial step temperature perturbations, the development and decay of the velocity and pressure perturbations being shown in figures 5 (*b*) and (*c*) respectively. The aim is to illustrate the decay of perturbations and the transition from a constant-density cooling process to a constant-pressure process in the presence of the magnetic field. For this purpose, we fixed $B^2 = 0{\cdot}1$ and plotted the perturbation profiles for various $\bar{\tau}$ in figure 5. The next step is to investigate the effects of increased strength of the magnetic field. To illustrate the strong magnetic field effects, we have also shown the profiles for $B^2 = 1$ at $\bar{\tau} = 5$ and for $B^2 = 10$ at $\bar{\tau} = 3$ in figure 5.

The perturbation profiles in figure 5 make it clear that the cooling process proceeds in a manner similar to that in the non-magnetic case. Olfe & DePlomb (1970) observe that the cooling proceeds with negligible motion and constant density at small times and dies out asymptotically at constant pressure at large times. At intermediate times gasdynamic waves appear travelling inwards and outwards from the temperature discontinuity. These modify the cooling considerably from what it would be if the entire decay were at constant density, with no induced velocities.

Even in the presence of the magnetic field, the cooling proceeds with negligible motion and constant density at small times and dies out at constant pressure at large times. At intermediate times gasdynamic waves travel with magneto-acoustic speeds inwards and outwards from the original temperature discontinuity

and modify the cooling process. We proceed to describe this cooling process and also understand how the strength of the magnetic field affects the above process with the help of the profiles in figure 5.

At small times the cooling proceeds with constant density and negligible motion as velocity perturbations are found to be small. We notice that the pressure perturbations vary rapidly in the vicinity of the temperature discontinuity (see the profiles in figure 5 (*c*) for $B^2 = 0{\cdot}1, \bar{\tau} = 0{\cdot}5, 1, 3$). These pressure perturbations are due to heating in the region $\eta > \eta_0$ and cooling in the region $n < \eta_0$ occurring at early times (figure 5 (*a*)). (The radiative transfer heats up the region $\eta > \eta_0$ more in the presence of the magnetic field than in its absence and thus the temperature profiles in figure 5 (*a*) look continuous even at early times.) These large pressure perturbations produce negative velocity pulses near $\eta = 0$ (see the profiles for $B^2 = 0{\cdot}1$, $\bar{\tau} = 0{\cdot}5$, 1, 3 in figure 5 (*b*)). As time progresses the pressure and velocity perturbations spread out to further distances from η_0. Then, heating and cooling waves produced by the gas motion travel inwards and outwards from the temperature discontinuity respectively with magneto-acoustic speed. As time progresses further the pressure pulses reach $\eta = 0$. The pressure increases near $\eta = 0$ in the region $\eta < \eta_0$ owing to the accumulation of gas and it decreases in the region $\eta_0 < \eta < 2\eta_0$ owing to loss of mass (see the profile for $B^2 = 0{\cdot}1$, $\bar{\tau} = 10$ in figure 5 (*c*)). These pressure changes are accompanied by corresponding velocity changes. The inward flow at $\eta = 0$ is reduced and there is appreciable inward flow away from $\eta = 0$ (see the profile for $B^2 = 0{\cdot}1$, $\bar{\tau} = 10$ in figure 5 (*b*)). The reduction in the negative pressure perturbation in the core (near $\eta = 0$) results in a reflected temperature wave originating from the far discontinuity $\eta = -\eta_0$ consisting of temperature perturbations closer to constant-pressure values (see the profile for $B^2 = 0{\cdot}1$, $\bar{\tau} = 10$ in figure 5 (*a*)). At later times the velocity and pressure perturbations decay to zero (see the profiles for $B^2 = 0{\cdot}1$, $\bar{\tau} = 25$ in figures 5 (*b*), (*c*)). Then the temperature perturbations decay with nearly constant-pressure values (see the profiles for $B^2 = 0{\cdot}1$, $\bar{\tau} = 25$ in figure 5 (*a*)).

As the cooling and heating waves produced by the gas motion travel with the velocity c_s, they reach $\eta = 0$ earlier in the presence of a stronger magnetic field. As a result, the pressure increase near $\eta = 0$ and the pressure decrease in the region $\eta_0 < \eta < 2\eta_0$ take place earlier. This can be noticed in figure 5 (*c*), where the increase in pressure near $\eta = 0$ and the decrease in pressure away from $\eta = 0$ occur at about the times $\bar{\tau} = 10$, 5 and 3 for $B^2 = 0{\cdot}1$, 1 and 10 respectively. Correspondingly we also notice in figure 5 (*b*) that appreciable reduction in the inward velocity in the core and increase of negative velocity at large distances from $\eta = 0$ occur at times $\bar{\tau} = 10$, 5 and 3 for the respective values of $B^2 = 0.1$, 1 and 10. Thereafter, the temperature perturbations start decaying at nearly constant pressure (see the profiles for $B^2 = 1$, $\bar{\tau} = 5$ and $B^2 = 10$, $\bar{\tau} = 3$ in figure 5 (*a*)).

Therefore, we conclude that the temperature perturbations attain constant-pressure cooling values earlier, i.e. in the presence of magnetic field the transition from a constant-density process to a constant-pressure process is more rapid. This is because the magnetic field causes faster decay of velocity and pressure perturbations.

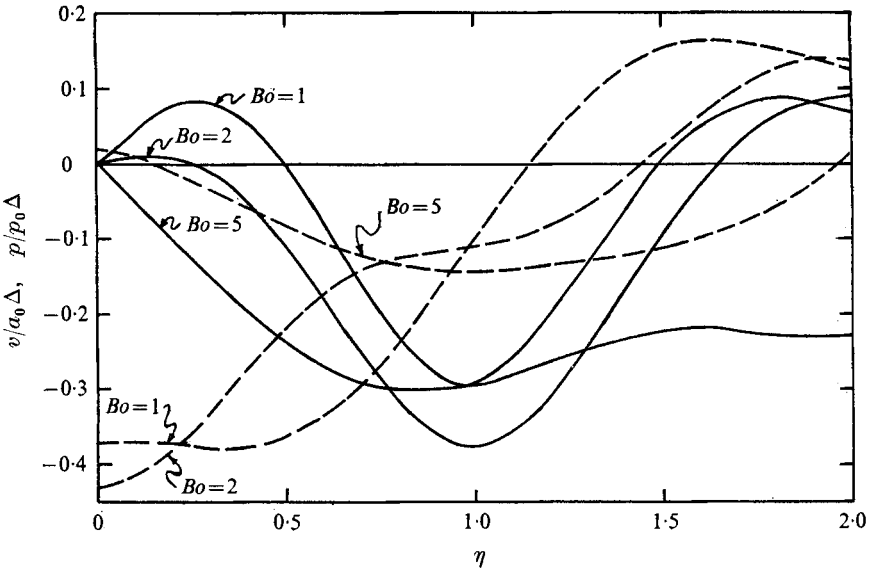

FIGURE 6. Velocity (solid line) and pressure (broken line) perturbation profiles with $2\eta_0 = 2, \bar{\tau} = 5, B^2 = 0{\cdot}1$ and $\gamma = \frac{5}{3}$, for $Bo = 1, 2, 5$.

Since the waves generated at the temperature discontinuities travel at the magneto-acoustic speed, they will reach the profile centre at time

$$\bar{\tau}^* = (16/Bo)\,\eta_0/(1+B^2)^{\frac{1}{2}}.$$

This expression for $\bar{\tau}^*$ also shows that the transition time decreases as B^2 is increased. The magnetic field hastens only the above transition of the cooling process and not the entire decay process. In fact, as was observed in the first paragraph of this section, the cooling time is longer than in the non-magnetic case and becomes progressively longer with the increasing strength of the magnetic field.

The induced non-dimensional velocity and pressure perturbations are appreciable for $Bo = 5$ as shown in figures 5 (*b*) and (*c*). In figure 6, the velocity and pressure perturbation profiles for $Bo = 1$, 2, and 5, $B^2 = 0{\cdot}1$, $\eta_0 = 1$ and $\bar{\tau} = 5$ are drawn. These perturbations increase with decreasing Bo and decay over progressively longer times as Bo decreases. For example, the velocity and pressure perturbations for $Bo = 1$ and 2 spread out further as time progresses before decreasing to zero. However, as observed earlier, the decay of these perturbations to zero depends on the strength of the magnetic field, which reduces their decay time.

In the present work the specific calculations have been carried out for the case of no initial perturbations in pressure and velocity. However, the development of magneto-acoustic waves and the transition from constant-density to constant-pressure cooling should be features of most cooling processes even when initial pressure and velocity perturbations exist.

REFERENCES

BALDWIN, B. S. 1962 *N.A.S.A. Tech. Rep.* R-138.

COGLEY, A. C. & VINCENTI, W. G. 1969 *J. Fluid Mech.* **49**, 641.

GOLITSYN, G. S. 1963 *Bull. Acad. Sci. USSR Geophys. Ser.* (English trans.) no. 589.

HELLIWELL, J. B. 1966 *Phys. Fluids*, **9**, 1869.

HELLIWELL, J. B. & NYE, V. A. 1969 *Quart. J. Mech. Appl. Math.* **22**, 453.

KOURGANOFF, V. 1952 *Basic Methods in Transfer Problems.* Oxford University Press.

LICK, W. 1964 *J. Fluid Mech.* **18**, 274.

MOORE, F. K. 1966 *Phys. Fluids*, **9**, 70.

NYE, V. A. 1970*a* *Quart. J. Mech. Appl. Math.* **23**, 265.

NYE, V. A. 1970*b* *Quart. J. Mech. Appl. Math.* **23**, 247.

OLFE, D. B. & DEPLOMB, E. P. 1970 *J. Fluid Mech.* **40**, 127.

PROKOF'EV, V. A. 1957 *Prikl. Math. Mech.* **21**, 775.

RIAZANTSEV, I. S. 1959 *Prikl. Math. Mech.* **23**, 1126.

SMITH, P. W. 1957 *J. Acoust. Soc. Am.* **29**, 693.

SOLAN, A. & COHEN, I. M. 1966 *Phys. Fluids*, **9**, 2365.

VINCENTI, W. G. & BALDWIN, B. S. 1962 *J. Fluid Mech.* **12**, 447.